Journal of Orthopaedic Translation 20 (2020) 47–55

Contents lists available at ScienceDirect

Journal of Orthopaedic Translation

journal homepage: www.journals.elsevier.com/journal-of-orthopaedic-translation

Original Article

Three-dimensional finite-element analysis of aggravating medial meniscus tears on knee osteoarthritis

Lan Li [a,b,☆], Longfei Yang [a,☆], Kaijia Zhang [b], Liya Zhu [c], Xingsong Wang [a,*], Qing Jiang [b,**]

[a] School of Mechanical Engineering, Southeast University, China
[b] State Key Laboratory of Pharmaceutical Biotechnology, Department of Sports Medicine and Adult Reconstructive Surgery, Drum Tower Hospital Affiliated to Medical School of Nanjing University, China
[c] School of Electrical and Automation Engineering, Nanjing Normal University, China

ARTICLE INFO

Keywords:
Meniscus tear
Finite-element simulation
Biomechanics
Osteoarthritis
Meniscectomy

ABSTRACT

Background: The biomechanical change during the medial meniscus damage in the process of knee osteoarthritis has not been explored. The purpose of this study was to determine the effect of aggravating medial meniscus degenerative tear on the progress of knee osteoarthritis through the finite-element simulation method.

Methods: The three-dimensional digital model of a total-knee joint was obtained using a combination of magnetic resonance imaging and computed tomography images. Four types of medial meniscus tears were created to represent the aggravating degenerative meniscus lesions. Meniscectomy of each meniscal tear was also utilized in the simulation. The compression and shear stress of bony tissue, cartilage, and meniscus were evaluated, and meniscus extrusion of the healthy knee, postinjured knee, and postmeniscectomy knee were investigated under the posture of balanced standing.

Results: Based on the results of finite-element simulation, the peak shear principal stress, peak compression principal stress, and meniscus extrusion increased gradually as the meniscus tears' region enlarged progressively (from 7.333 MPa to 15.14 MPa on medial femur and from 6 MPa to 20.94 MPa on medial tibia). The higher stress and larger meniscus extrusion displacement in all tests were observed in the flap and complex tears. The oblique tears also had a biomechanical variation of stress and meniscus extrusion in the knee joint, but their level was milder. Both the peak value of the stress and meniscus displacement increased after the meniscectomy.

Conclusion: In contrast to the damaged hemijoint, the stress applied on the healthy lateral hemijoint increased. The change of biomechanics was more obvious with the aggravation of meniscus injury. The advanced degenerative damage resulted in increasing stress that was more likely to cause symptomatic clinical manifestation in the knee joint and accelerate the progress of osteoarthritis. Moreover, we found that the meniscus injury caused higher stress concentration on the contralateral side of the joint. We also discovered that the meniscectomy can lead to more serious biomechanical changes, and although this technique can relieve pain over a period of time, it increased the risk of osteoarthritis (OA) occurrence.

The translational potential of this article: It is clear that the meniscal lesions can cause osteoarthritic knee, but the biomechanical change during the meniscus damage period has not been explored. We have evaluated the variation of stress during the aggravating medial degenerative meniscus tears and the relationship in the process of knee OA through finite-element simulation. This study does favour to obtain a better understanding on the symptoms and pathological changes of OA. It also may provide some potential directions for the prophylaxis and treatment of OA.

* Corresponding author. School of Mechanical Engineering, Southeast University, No.2 Southeast University Road, Nanjing, China.
** Corresponding author. Department of Sports Medicine and Adult Reconstructive Surgery, Drum Tower Hospital Affiliated to Medical School of Nanjing University, Nanjing, China.
E-mail addresses: xswang@seu.edu.cn (X. Wang), qingj@nju.edu.cn (Q. Jiang).
☆ Lan Li and Longfei Yang are cofirst authors, and they contributed equally to the work.

https://doi.org/10.1016/j.jot.2019.06.007
Received 28 March 2019; Received in revised form 11 June 2019; Accepted 28 June 2019
Available online 7 August 2019

Introduction

The menisci act as load sharers and shock absorbers in the knee joint, and the biomechanical effect of the loss of meniscal function has been well explored [1–3]. Meniscal tears are exceedingly common and generally accompanied by disruption of the hoop fibres, resulting in meniscus extrusion, dislodging, and interarticular narrowing under the applied axial load [4]. Based on the type of the inducement of meniscus tears, the damage can be divided into traumatic and degenerative lesions. The degenerative lesions exhibit a higher incidence but are asymptomatic in the early stages. According to some studies on large samples, more than 50% of the participants with degenerative meniscus tears did not have knee symptoms, whereas the ratio increased to more than 90% in patients with symptomatic osteoarthritis (OA), in whom a meniscus tear was found [5–7]. This type of lesions is commonly described as horizontal cleavages, oblique, flap, or complex tears, which are associated with ageing, preexisting, or incipient osteoarthritic disease [8–10]. Owing to the mild, frequently painless symptoms, the degenerative lesions are easy to neglect at an early stage, although the negative effect on the knee biomechanics already exists. Accompanied by aggravation of the meniscus tears, such as the oblique tear and flap tear, and finally by a complex tear, the irregular biomechanical balance is worsened. Indeed, the degenerative meniscal tears play a momentous role in the early stage of knee OA, although they do not directly result in knee pain [11]. The typical degenerative tears, including the oblique, flap, and complex tears, generally occur in the avascular body portion, and thus, the healing rates are poor [12,13]. Meniscectomy has been widely performed to treat such meniscus tears. However, the long-term clinical follow-up has demonstrated a high incidence of knee dysfunction and tissue degeneration [14].

An explicit understanding of the stress transmission in the intra-articular space during the aggravating meniscus degenerative tears and postmeniscectomy may facilitate the exploration of the biomechanical aetiology of the progress of OA. The finite-element (FE) simulation can provide intuitive graphical results to explain the biomechanical changes in the knee joint induced by meniscal tears and meniscectomy. Several two-dimensional (2D) or three-dimensional (3D) computational models of the knee joint have been developed earlier to analyze the effect of meniscus tears and meniscectomy on the knee biomechanical behaviour [2,3,15,16]. Almost all these examinations have documented the changes caused by the contact stress on the contact area of the connective tissues. Therefore, it has been assumed that the bone structures are to be considered rigid bodies because the Young's modulus of the bone is much higher than that of the menisci, ligaments, and cartilages, and hence the deformation of the bone can be ignored. This concept is correct from a mechanical standpoint, but from a pathophysiological viewpoint, the stress applied on the femur and tibia should be taken into account. As mentioned previously, the stress concentration and the microfracture of the subchondral bone are correlated with damage of the cartilage and the development of knee OA [17,18]. Elucidation of the impact of the stress transformation on the bone tissue of the postinjured knee would systematically expand our understanding of the progress of OA.

We hypothesized that the overload in the knee will aggravate as the damage area in the meniscus increases, and this phenomenon can induce the course of OA. To investigate the influence of meniscus degenerative lesions and the related subsequent meniscectomy on the change of knee biomechanics, a 3D FE model of the knee joint was developed based on the combination of magnetic resonance imaging (MRI) and computed tomography (CT) images. We introduced four aggravating degenerative tears (small oblique tear, big oblique tear, flap tear, and complex tear) on the medial meniscus (Figure 1A). Vertical force was applied on the model to simulate the balance standing posture. In addition, meniscectomy of each tear (Figure 1B) was also simulated under the action of the vertical force. According to the introduction to the common procedures of meniscectomy [19], the tear region occurred in the poor vascular supply should be commonly excised or removed entirely. The damage region on the meniscus is generally trimmed to a smooth peripheral rim, while the largest volume of the meniscus is preserved to reduce the risk of degenerative arthritis. Finally, the compression stress and the shear stress on the bone and cartilages were estimated to evaluate the effect of the meniscus tears and meniscectomy on the knee joint biomechanics and OA progress.

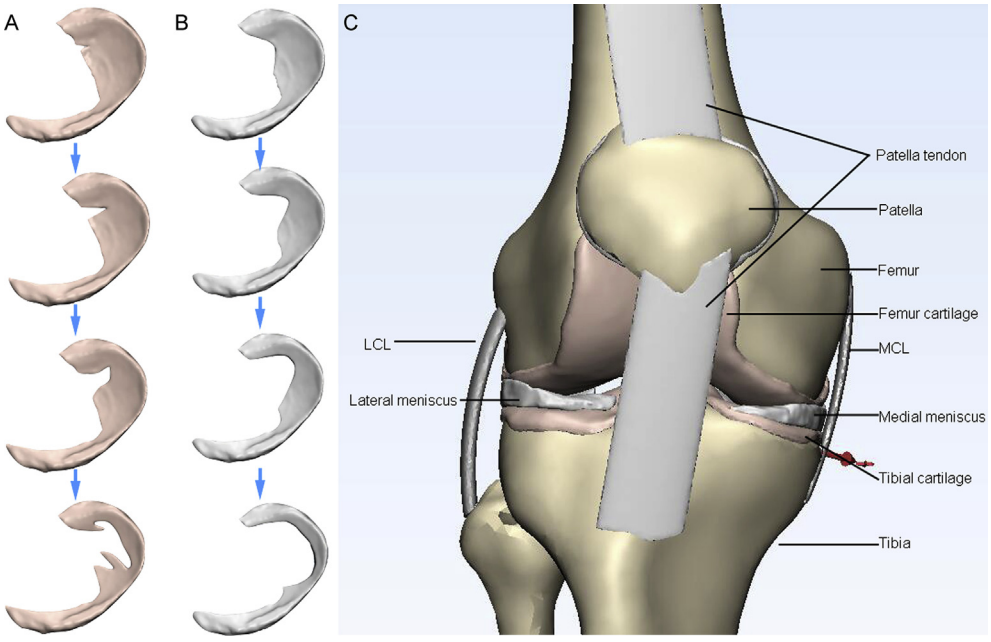

Figure 1. View of the 3D models used in the FE simulation. (A) Aggravating degenerative medial meniscus tear models: from top to bottom: small oblique tear, big oblique tear, flap tear, and complex tear. (B) The related meniscectomy models of each meniscus tear. (C) A general view of the knee joint model. 3D = three-dimensional; FE = finite-element.

Methods

Data acquisition

The magnetic resonance data were obtained from a 35-year-old healthy male volunteer with a body weight of 80 kg and a height of 178 cm by a 3-T clinical MR scanner (uMR 770; United Imaging, Shanghai, China) using the 12-channel knee send-receive radio frequency coil. The volunteer neither had any underlying diseases nor lower limb traumatic history. The volunteer was placed in a supine position with no weight-bearing, and the knee to be examined was positioned in the central region of the coil. A modulated flip angle technique in refocused imaging with extended echo train sequence was performed in each participant using 2 excitations and 176 contiguous slices, and a slice thickness of 1.5 mm, repetition time 1000 ms, echo time 56 ms, matrix 240 × 228, field of view 152 mm, and voxel size 0.67 × 0.63 × 0.64 mm^3 were used in sagittal planes. The scan time was 6 min and 44 s. A CT scan was performed using a GE Lightspeed 16 CT equipment (GE Healthcare, CT, USA) on the same participant on the lower limb at the neutral posture with a slice distance of 0.625 mm and a field of view of 500 mm.

Three-dimensional reconstruction and combination of the knee joint

The 3D reconstruction was performed by MIMICS 19.0 (Materialise, Leuven, Belgium). The separated 3D reconstruction of the bone structures was accomplished with CT bone segmentation operation. The contours of the articular cartilages (femoral, tibial, and patellar), menisci (medial and lateral), and ligaments (medial collateral, lateral collateral, anterior cruciate, posterior cruciate, and patellar tendon) were segmented from the MRI images. The manual segmentation process of the nonbony structures was performed under the supervision of an experienced orthopaedist and radiologist at an accuracy of 0.1 mm to minimize the variation in the models. Four types of meniscus tears and the related meniscectomy models were created by Magics 19.0 (Materialise).

FEM modelling and material properties

All the data were exported as stereolithography (STL) files and remeshed in 3-matic 11.0 software (Materialise). The completed models were imported and assembled in the Abaqus 2017 (SIMULIA, Rhode Island, USA), the general view of which is displayed in Figure 1C. As the ligaments are nonlinear materials, the quadratic hybrid formulation was used and the type of unit was a 10-node quadratic tetrahedron (C3D10H). For other linear materials, the common 4-node linear tetrahedron (C3D4) unit was used in this study.

The ligaments were modelled as transversely isotropic nearly incompressible neo-Hookean materials [2,20] using the strain energy function:

$$\Phi = C_1(\overline{G_1} - 3) + \frac{1}{D_1}(J_F - 1)^2 + S(\lambda)$$

Here, $S(\lambda)$ represents the strain energy function of the fibre family which satisfies the following conditions:

$$\lambda\frac{dS}{d\lambda} = \begin{cases} 0, & \lambda \le 1 \\ C_3\left(e^{(\lambda-1)C_4} - 1\right), & 1 < \lambda < \lambda^* \\ C_5\lambda + C_6, & \lambda \ge \lambda^* \end{cases}$$

C_1 is a bulk material constant related to the shear modulus μ ($C_1 = 2/\mu$). J_F is the Jacobian matrix of the deformation gradient F, and $\overline{G_1}$ denotes the first invariant of the left Cauchy–Green tensor $\overline{G_1} = tr\overline{F}\overline{F}^T$ with the modified deformation gradient $\overline{F}$ ($\overline{F} = J_F^{-0.33}F$).

The stress in the fibres was dependent on the fibre stretch λ, which is determined from the deformed fibre orientation $\mathbf{a_d}$, the deformation gradient $\mathbf{F}$, and the initial fibre orientation $\mathbf{a_0}$ ($\lambda \cdot \mathbf{a_d} = \mathbf{F} \cdot \mathbf{a_0}$). Under compression of $\lambda \le 1$, the fibres did not support any compressive stresses. It is noteworthy that the stiffness of the fibres increased exponentially when the fibre stretch was within the range from 1 to the predefined value (λ^*). Beyond this stretch, the fibres straightened and the stiffness increased linearly. The constant C3 scales the exponential stress, C4 is related to the rate of collagen uncramping, and C5 represents the elastic modulus of the straightened collagen fibres. The constant C6 was introduced to ensure stress continuation at $\lambda^*[C_6 = (e^{C_4(\lambda^*-1)} - 1)\cdot C_3 - (C_5\lambda^*)]$. The values of the material constants C_1, C_3, C_4, C_5, and D_1 are listed in Table 1.

The bone material behaviour was linear, with an elastic modulus (E) as of 7300 MPa and a Poisson ratio (ν) of 0.3 [21]. The articular cartilage and the menisci were assumed to be composed by a single-phase linear elastic and isotropic material. The average material properties for the aforementioned two connective tissues were E = 15 MPa, $\nu = 0.475$, and E = 120 MPa, $\nu = 0.45$, respectively [22–24].

Loads and boundary conditions

We included the total tibiofemoral joint in the realistic knee joint characterization, and three FE simulations were designed based on the balanced standing posture. The numerical value of force was set based on the studies of Ahmed and McLean [25] and Heller et al [26]. The boundary conditions are defined as follows. The tibia and fibula were fixed in all translations and rotations because the femur was unconstrained in all translational and rotational degrees of freedom. All the ligaments were rigidly attached to their corresponding bones to simulate the bone–ligament attachment. The muscles around the knee joint were not included in the simulation. The kinematic constrain was modelled between the femur and the meniscus, the meniscus and the tibia, and the femur and the tibia in the joint. The contact area between cartilage and menisci was decreased as the damage area increases. For the balanced standing simulation, a vertical compressive load of 1150 N was applied on the femur at 0° of flexion. The meniscectomy was also completed using the condition of balanced standing simulation.

Results

Balanced standing simulation

The numerical values of the peak compression and the shear stress were increased in the postinjured knee joint (Figure 2). Among the four meniscus tears, the flap and complex tears exerted higher compression and shear stress on the medial femur and meniscus, but no obvious difference was found on the cartilages and tibia. For the healthy hemijoint, the peak compression principal stress was similar among bony tissues and cartilage, but the value was higher in the meniscus of flap tear and complex tear. The peak shear stress of the flap and complex tears on the lateral femur was higher than that induced by the oblique tears, and the meniscus with the complex tear had the highest. No obvious difference in the shear stress can be observed in lateral cartilages and tibia. This finding indicates that the flap and complex tear result in a more serious

Table 1
Material constants of the ligaments.

	C_1 (MPa)	C_3 (MPa)	C_4 (–)	C_5 (MPa)	D_1 (MPa^{-1})	λ^* (–)
ACL	1.95	0.0139	116.22	535.039	0.00683	1.046
PCL	3.25	0.1196	87.178	431.063	0.0041	1.035
LCL	1.44	0.57	48.0	467.1	0.00126	1.063
MCL	1.44	0.57	48.0	467.1	0.00126	1.063
PT	3.25	0.1196	87.178	431.063	0.0041	1.035

ACL = anterior cruciate ligament; PCL = posterior cruciate ligament; LCL = lateral collateral ligament; MCL = medial collateral ligament; PT = patellar tendon.

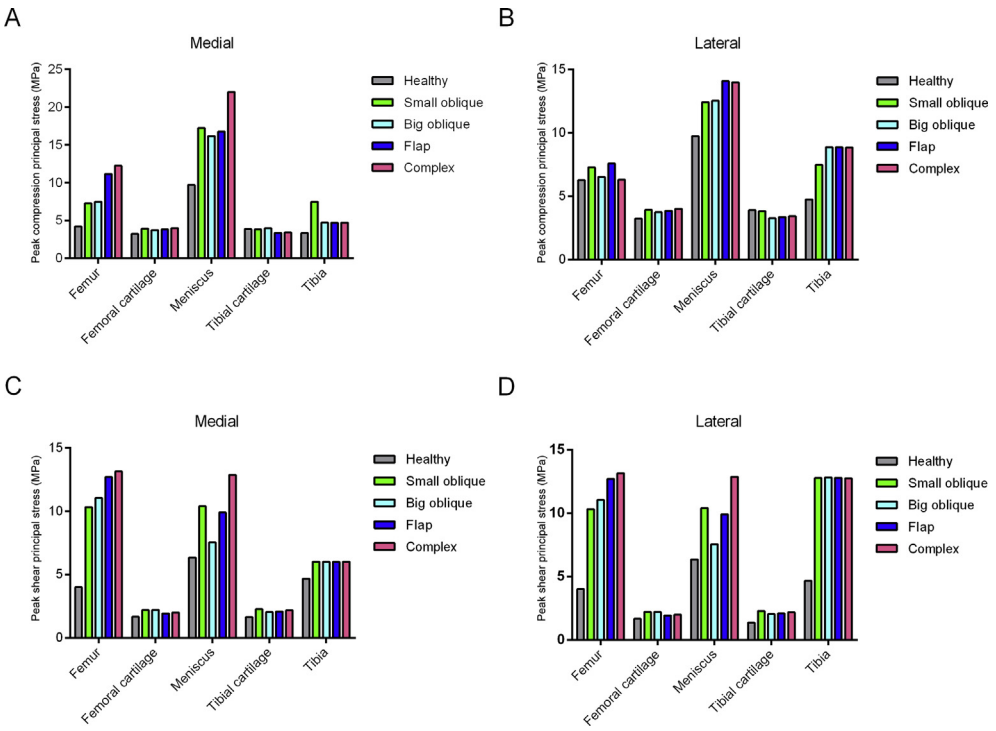

Figure 2. Maximum peak compression and shear stress applied on the knee joint in the balanced standing simulation. (A) The maximum peak compression principal stress in the medial hemijoint; (B) the maximum peak compression principal stress in the lateral hemijoint; (C) the maximum peak shear principal stress in the medial hemijoint; (D) the maximum peak shear principal stress in the lateral hemijoint.

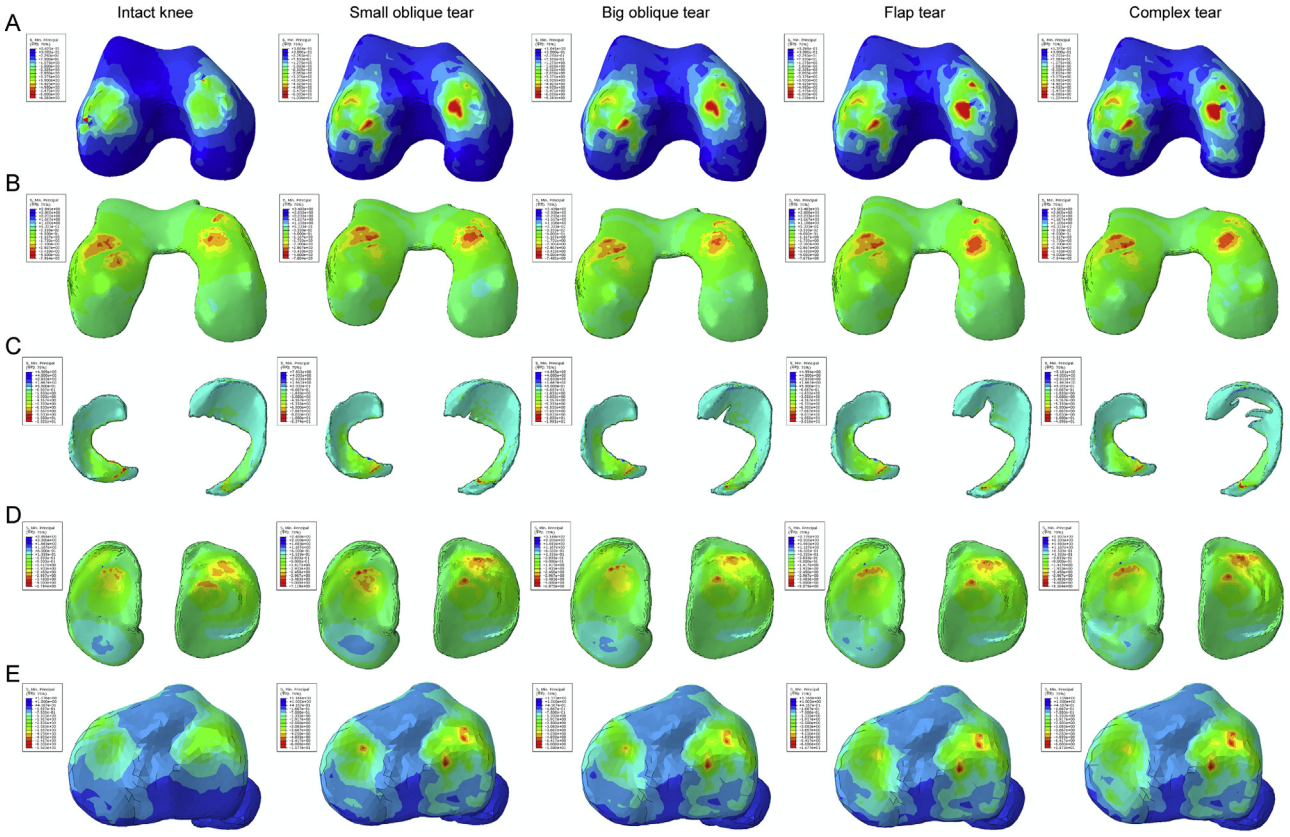

Figure 3. The results of compression stress (min principal stress) in the balanced standing simulation. The colour changes from red to deep blue represent the stress variation from large to small on the stress nephogram. From top to bottom: (A) femur, (B) femur cartilage, (C) menisci, (D) tibial cartilage, and (E) tibia.

overloading in the balance standing posture.

For the compression stress distribution on Figure 3, we can find that the red colour appeared on both sides of bony tissues after the occurring of meniscus tear, and the area of green and indigo was also increased gradually, especially in the medial hemijoint, indicating that the high compression stress region was enlarged as the tears were aggravated. The same change can be seen on cartilages either; although the numerical values of the peak compression principal stress remained similarity, the area of red, green, and indigo increased, representing that the cartilages undertook higher compression stress after the meniscus were damaged. Meanwhile, the colour distribution on meniscus was close to each other.

The distribution of the shear stress is illustrated in Figure 4, and they displayed the same variation tendency with the compression stress; the shear stress on bony tissues was increased notably as the meniscus was injured. The areas of red and green on the medial hemijoint were obviously larger in the flap and complex tear. They also exhibited a phenomenon of increased area on lateral tibia. Still, the meniscus of each group gained the same shear stress distribution tendency. From the variation of numerical values and high compression regions, we can conclude that the complex tear and flap tear result in a worse biomechanical change in the knee joint.

The properties of the extrusion displacement are presented in Table 2. The medial meniscus displacement was approximately 1.8 mm, and the lateral meniscus displacement was around 2.7 mm. The displacement increased in the flap and complex tears on both sides of the meniscus, but only lateral meniscus extrusion was observed in the oblique tears.

Meniscectomy simulation

The change in the shear stress distribution was exhibited distinctly in the stress nephogram (Figure 5). All the meniscectomy models showed enlargement of the high shear stress–affected area on bones and cartilages in comparison with the related meniscus tear models. In detail, a notable area increase of red and green can be found on medial condyle of the femur, and the correlated articular surface on femur cartilage showed that the shear stress on these regions was raised. In addition, the colour on the medial posterior horn of the tibial cartilage turned from blue and indigo to green as the meniscus tears were aggravated, and a larger area of green can be observed on the lateral tibia. The colour distribution area on the meniscus obtained no obvious variation. The compression stress distribution (Figure 6) demonstrated the similar change tendency to the shear stress.

Table 2
Meniscus extrusion in the balanced standing simulation (mm).

	Healthy	Small oblique	Big oblique	Flap	Complex
Medial	1.801	1.788	1.791	1.921	1.962
Lateral	2.641	2.754	2.715	2.749	2.796

The numerical values of the peak compression principal stress and peak shear principal stress are shown in Figure 7A and B. The values on bony tissues and cartilages showed no distinct difference within different resection areas. But a notable difference appeared on the meniscus; the smallest resection area led to the smallest peak value of stress. In Figure 7C to F, the variation of peak shear stress and peak compression principal stress before and after meniscectomy is shown. It is obvious that all the values on all components increased after meniscectomy.

Except for the enlarged shear stress, meniscus extrusion was promoted in all kinds of meniscectomy (Table 3). The meniscectomy after the complex tear showed the largest displacement, and the extrusion was exacerbated by the increase in the resection area.

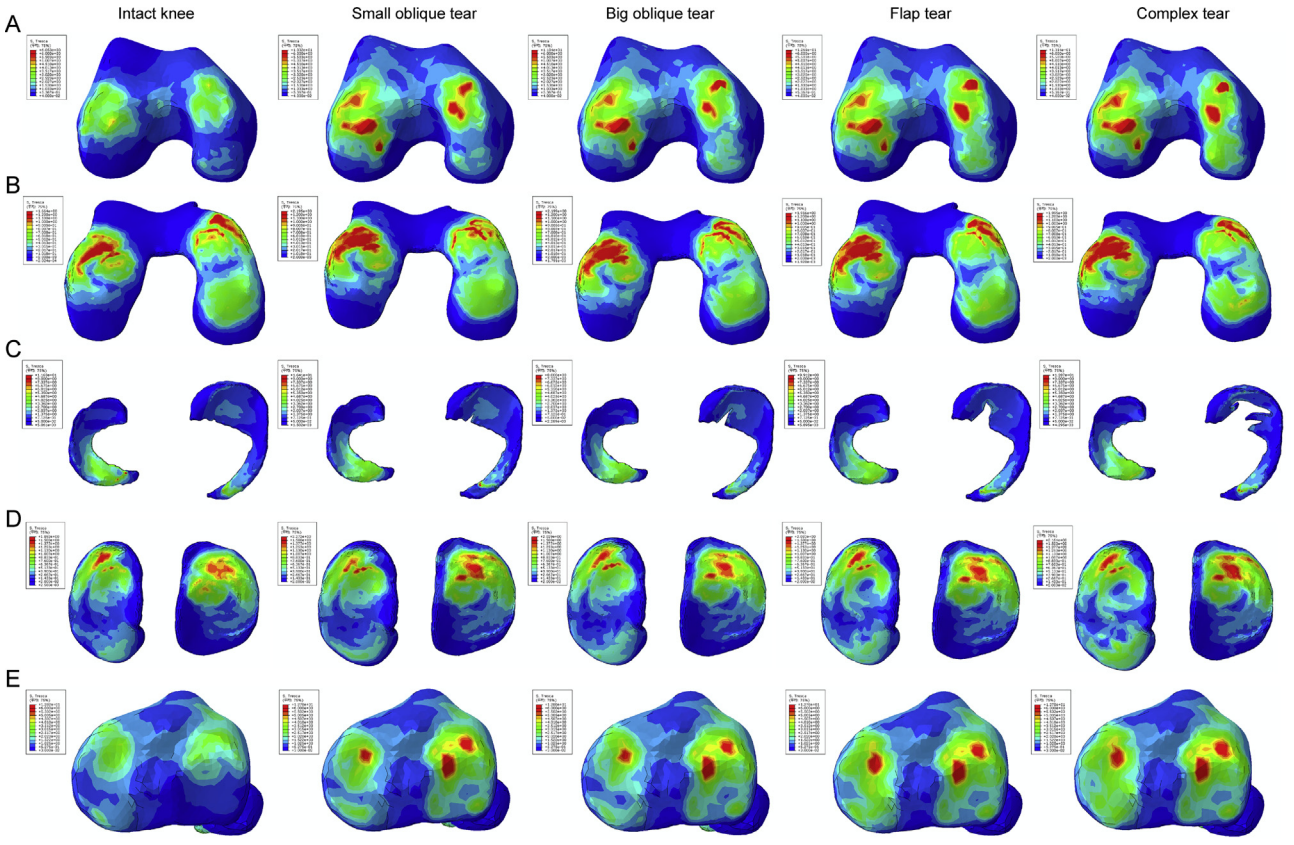

Figure 4. The results of the shear stress (Tresca stress) in the balanced standing simulation. The colour changes from red to deep blue represent the stress variation from large to small on the stress nephogram. From top to bottom: (A) femur, (B) femur cartilage, (C) menisci, (D) tibial cartilage, and (E) tibia.

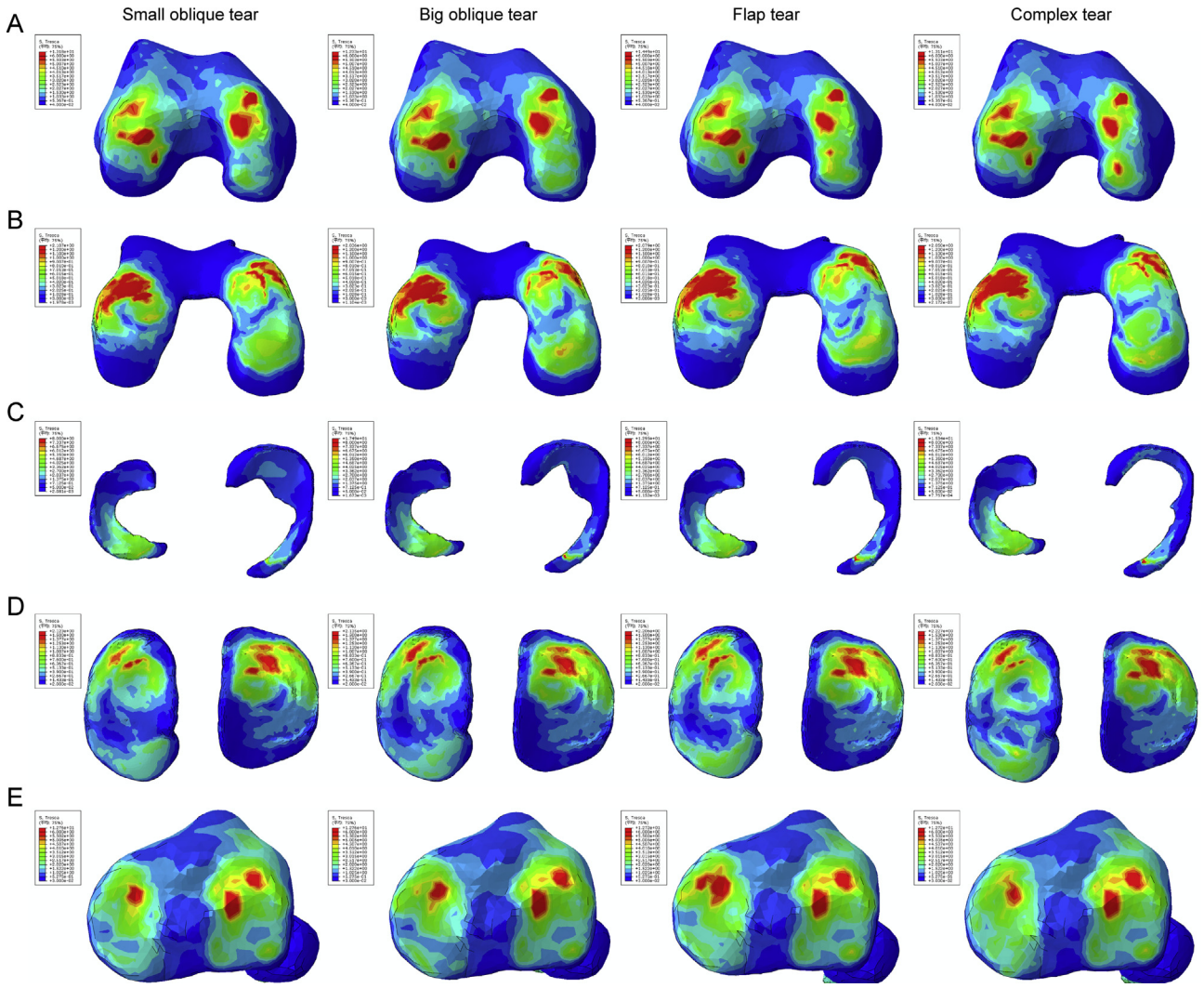

Figure 5. The results of the shear stress (Tresca stress) in the meniscectomy simulation. The colour changes from red to deep blue represent the stress variation from large to small on the stress nephogram. From top to bottom: (A) femur, (B) femur cartilage, (C) menisci, (D) tibial cartilage, and (E) tibia.

Discussion

In this study, a realistic computational FE model of the total-knee joint was developed to evaluate the intraarticular changes in the biomechanical behaviour after meniscus tears and meniscectomy. The results of our FE simulation concerning the stress on the meniscus of the intact knee were similar to those of previous studies, indicating that the analytical results obtained by the use of the model used in this study are reliable [1,2,16,20,27]. The FE simulation demonstrated the instantaneous response of the knee joint under the compression load induced, but the tendency observed herein indicates the potential impact of the biomechanical changes on the progress of knee OA. Under the balanced standing simulation, we found that the meniscus extrusion in the lateral side was larger than that in the medial side because of the difference in the load bearing between the compartments. Insignificant differences were established among the different groups.

The meniscus extrusion was aggravated by the gradually increasing severity of the tear, and the meniscectomy resulted in further deterioration of the meniscus extrusion, which was confirmed by the clinical manifestation observed. The disruption in the hoop fibres of the meniscus might be the cause for this phenomenon, resulting in damage of the inherent structure of the meniscus. Subsequently, these unfavourable changes lead to a decline in the hoop strength, which plays a vital role in resisting meniscus extrusion under loading [9,28]. The normal morphology of the meniscus was difficult to preserve under the load applied and after the tears in the meniscus occurred, which narrowed the joint space. It is generally known that joint-space narrowing (JSN) is one of the main bony features of the progress of OA [29]. Based on the results of our study, we can deduce that JSN may appear after a serious degenerative meniscus tear has occurred, such as flap and complex tears. Moreover, although meniscectomy can relieve the symptoms, the effect on the knee biomechanics is much worse than the meniscus tear itself. The overloading on the knee increases, which is accompanied by exacerbated JSN. The medial JSN results in the varus malalignment and the shift of the load-bearing axis, and the load in the medial hemijoint increases at this situation. During the balance standing posture, the adduction moment leads to the disproportionate medial transmission of load and greatly increases the risk of progress of OA [30]. On the other hand, a clinical study and an in vivo animal study have proved that the loss of meniscus volume is correlated with the exacerbating of JSN [31,32], indicating that the aggravating medial meniscus tears bring about the JSN and the alignment passing in the medial compartment and subsequent overload in medial hemijoint.

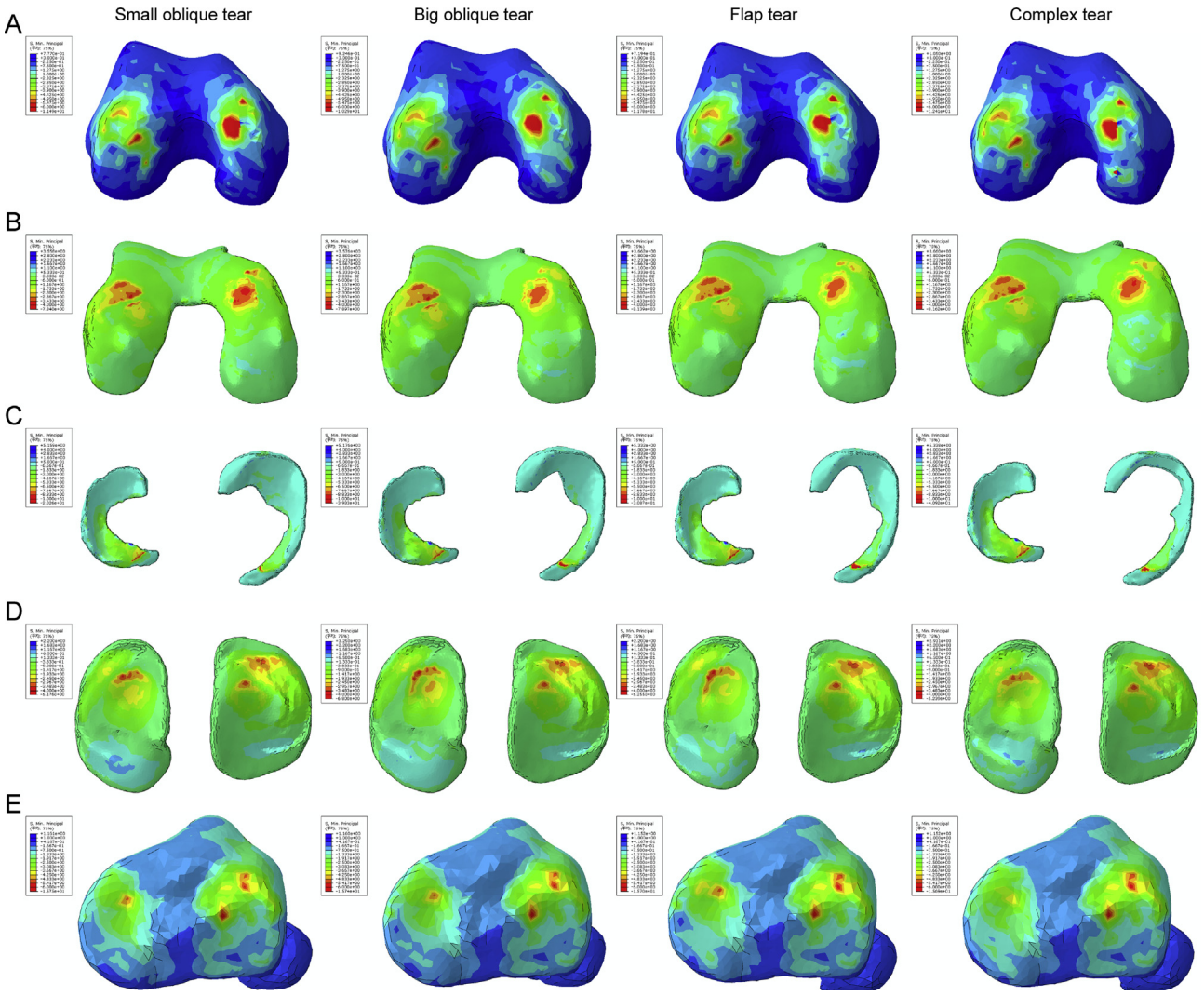

Figure 6. The results of compression stress (min principal stress) in the meniscectomy simulation. The colour changes from red to deep blue represent the stress variation from large to small on the stress nephogram. From top to bottom: (A) femur, (B) femur cartilage, (C) menisci, (D) tibial cartilage, and (E) tibia.

This, in turn, causes much more grievous JSN and probably leads to the beginning of a vicious circle that accelerates the progress of OA.

Besides JSN, a notable increase in the overload can be introduced by the meniscectomy, especially on the subchondral bone of the femur and tibia, which has been largely neglected in previous studies. In all the simulations of our examination, the shear stress applied on the medial femur and tibia was prominently elevated in the treatments with the flap and complex tears, which were considered to be the most serious among all four types of tears studied herein. Furthermore, the peak shear stress on the meniscus with the complex tear was obviously the highest in all the models, and a slight rise in the value was observed on the cartilages. Based on the results of the stress nephogram and the histogram, we can conclude that the shear stress increased along with the gradually deteriorating meniscus tear and achieved its peak value after the meniscectomy. Higher shear stress may result in early proteolytic degradation of the meniscal matrix and the articular cartilage and a decreased tensile strength [33,34]. The concentration of the shear stress directly indicates the risk region that may be damaged because of the abnormal overloading. In addition, the highest numerical value appeared in the meniscectomy models. The reason for this phenomenon may be the decrease of the contact area between the meniscus and the cartilages and the decline of the equivalent strength of the damaged meniscus [35]. Our findings are consistent with those of previous studies, confirming that the meniscal dysfunction increases the peak and average stress in the injured compartment, which may further facilitate the progress of OA [36].

Except the injured knee compartment, the peak compression and shear stress were also augmented in the healthy hemijoint. The damage of the medial meniscus and the decrease of the stiffness result in enlarging deformation and increased stress in the lateral meniscus, which may also lead to augmentation of the stress applied on the cartilages and the bone structures. Based on the clinical radiological data, the X-ray examination and 3D reconstruction (Figure 8A and B) revealed that obvious JSN occurred in the medial compartment of the knee at the advanced stage of OA, and severe osteophytes emerged around the articular surface. The routine T1-weighted MRI result (Figure 8C) clearly showed the cartilage damage on both sides of the knee joint, and cystic degeneration appeared in the medial femur and tibia, which are closely related to the progress OA and corroborate the results of the simplified model [37,38].

The menisci always bear an extremely high stress in every posture of the gait cycle. The meniscus tear in a healthy knee may eventually result in the occurrence of knee OA due to the meniscus dysfunction and the consequent overloading in the intraarticular space [39,40]. According to the results of previous case–control studies, OA is more likely to occur in a knee with meniscal tears but without cartilage lesions than in a knee with an intact meniscus, indicating that the meniscal tear comes before

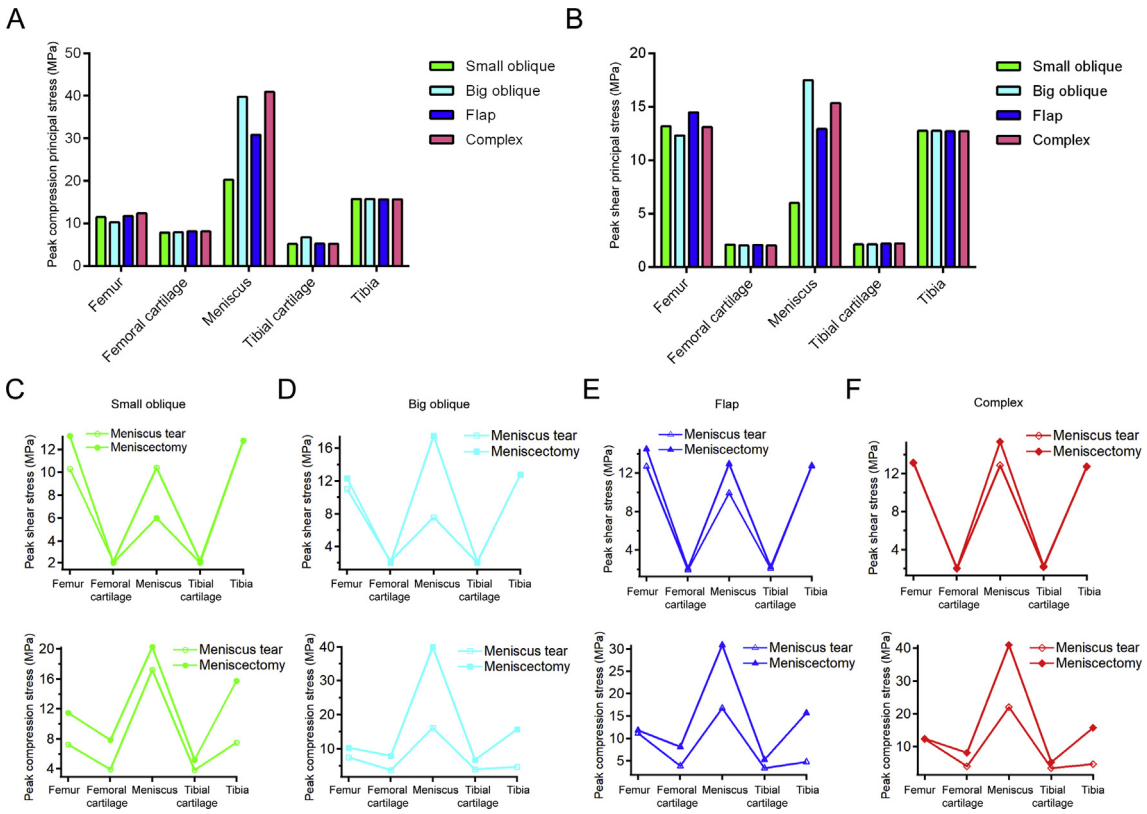

Figure 7. The results of stress variation in the meniscectomy simulation. (A) The peak compression principal stress; (B) peak shear principal stress after meniscectomy; (C) the variation of shear stress and compression stress before and after meniscectomy in small oblique tear; (D) the variation of shear stress and compression stress before and after meniscectomy in big oblique tear; (E) the variation of shear stress and compression stress before and after meniscectomy in flap tear; (F) the variation of shear stress and compression stress before and after meniscectomy in complex tear.

Table 3
Meniscus extrusion in the meniscectomy simulation (mm).

	Small oblique	Big oblique	Flap	Complex
Medial	1.877	1.922	2.089	2.195
Lateral	2.572	2.579	2.616	2.634

any visible cartilage changes can be noted [33,41]. The findings of our study also confirmed that notion; at the early stage of the meniscus degeneration, the high stress distribution area was not notably increased, but the situation probably began to change because much of the functionality of the meniscus was lost because of the tear and the related surgical resection [33]. The appearance of overloading on the cartilages and bones may expedite the process of OA. More importantly, according to the numerical value of the stress experienced and the meniscus displacement calculated by the FE simulation, the occurrence of OA in patients who underwent meniscectomy may be earlier than in patients with untreated meniscus degenerative tears. Perhaps, the implantation an artificial meniscus is a much more effective way to alleviate the pain and restore the knee function [42].

Some limitations exist in this study. First and foremost, we just analysed the stress variation in the computational models, and the biomechanical testing on human cadaver samples is missing, which can reflect the change of load and meniscus extrusion distinctly. Another limitation is the lack of clinical outcomes; the retrospective study of the relationship

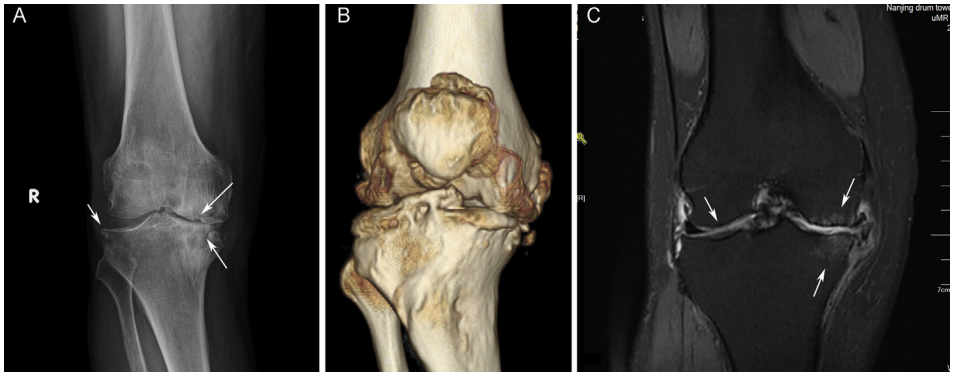

Figure 8. The clinical radiological data. (A)The X-ray and (B) 3D reconstruction results of a 62-year-old male patient; the medial compartment of the knee is markedly narrowed. (C) The MRI result of a 49-year-old female patient; subchondral bone osteonecrosis and cystic degeneration can be observed in the medial femur and tibia, as well as cartilage damage in both sides of the knee. 3D = three-dimensional; MRI = magnetic resonance imaging.

between different levels of medial meniscus tear and OA progression can strongly support our conclusion.

Conclusion

Using a realistic total-knee FE model, we have explored the biomechanical changes under aggravating degenerative meniscus tear and after meniscectomy. To simulate the stress transmission process, the bone structures were used in the FE simulation. Our results revealed that the peak shear principal stress and peak compression principal stress increased as the tear region gradually expanded and further increased after meniscectomy. The tendency in the changing of the stress and meniscus extrusion may explain the absence of symptoms in the early stage of meniscus degeneration and how the overloading affects the knee joint, inducing OA at an advanced stage of meniscus degeneration. In addition, we also found that meniscectomy exerted a negative effect on the knee biomechanics although it is still the most commonly used treatment option after meniscus tears.

Funding/support

This study was not supported by any funding.

Conflicts of interest

The authors have no conflicts of interest relevant to this article.

Acknowledgement

This study was supported by the International Cooperation and Exchange of National Natural Science Foundation (NSFC 81420108021), Key Program of NSFC (81730067), NSFC (51575100, 51705259), Postgraduate Research & Practice Innovation Program of Jiangsu Province (SJKY19_0061), Jiangsu Provincial Key Medical Center Foundation, and Jiangsu Provincial Medical Outstanding Talent Foundation.

References

[1] Peña E, Calvo B, Martínez MA, Doblaré M. A three-dimensional finite element analysis of the combined behavior of ligaments and menisci in the healthy human knee joint. J Biomech 2006;39:1686–701.
[2] Peña E, Calvo B, Martínez MA, Palanca D, Doblaré M. Finite element analysis of the effect of meniscal tears and meniscectomies on human knee biomechanics. Clin Biomech 2005;20:498–507.
[3] Dong Y, Hu G, Dong Y, Hu Y, Xu Q. The effect of meniscal tears and resultant partial meniscectomies on the knee contact stresses: a finite element analysis. Comput Methods Biomech Biomed Eng 2014;17:1452–63.
[4] Adams JG, Mcalindon T, Dimasi M, Carey J, Eustace S. Contribution of meniscal extrusion and cartilage loss to joint space narrowing in osteoarthritis. Clin Radiol 1999;54:502–6.
[5] Englund M, Guermazi A, Gale D, Hunter DJ, Aliabadi P, Clancy M, et al. Incidental meniscal findings on knee MRI in middle-aged and elderly persons. N Engl J Med 2008;359:1108.
[6] Bhattacharyya T, Gale D, Dewire P, Totterman S, Gale ME, Mclaughlin S, et al. The clinical importance of meniscal tears demonstrated by magnetic resonance imaging in osteoarthritis of the knee. J Bone Joint Surg Am 2003;85-A:4.
[7] Ding C, Martelpelletier J, Pelletier JP, Abram F, Raynauld JP, Cicuttini F, et al. Meniscal tear as an osteoarthritis risk factor in a largely non-osteoarthritic cohort: a cross-sectional study. J Rheumatol 2007;34:776–84.
[8] Poehling GG, Ruch DS, Chabon SJ. The landscape of meniscal injuries. Clin Sports Med 1990;9:539–49.
[9] Englund M, Guermazi A, Lohmander LS. The meniscus in knee osteoarthritis. Rheum Dis Clin N Am 2009;35:579.
[10] Englund M, Roemer FW, Hayashi D, Crema MD, Guermazi A. Meniscus pathology, osteoarthritis and the treatment controversy. Nat Rev Rheumatol 2012;8:412.
[11] Englund M, Niu J, Guermazi A, Roemer FW, Hunter DJ, Lynch JA, et al. Effect of meniscal damage on the development of frequent knee pain, aching, or stiffness. Arthritis Rheumatol 2014;56:4048–54.
[12] Stärke C, Kopf S, Petersen W, Becker R. Meniscal repair. Arthrosc J Arthrosc Relat Surg 2009;25:1033–44.
[13] Laible C, Stein DA, Kiridly DN. Meniscal repair. J Am Acad Orthop Surg 2013:204–13.
[14] Mcnicholas MJ, Rowley DI, Mcgurty D, Adalberth T, Abdon P, Lindstrand A, et al. Total meniscectomy in adolescence. A thirty-year follow-up. J Bone Joint Surg Br 2000;82:217.
[15] Venäläinen MS, Mononen ME, Jurvelin JS, Töyräs J, Virén T, Korhonen RK. Importance of material properties and porosity of bone on mechanical response of articular cartilage in human knee joint–a two-dimensional finite element study. J Biomech Eng 2014;136. 121005-121005.
[16] Ji YB, Park KS, Seon JK, Dai SK, Jeon I, Song EK. Biomechanical analysis of the effects of medial meniscectomy on degenerative osteoarthritis. Med Biol Eng Comput 2012;50:53–60.
[17] Buckland J. Osteoarthritis: subchondral bone erosion in hand OA: insights into the role of inflammation. Nat Rev Rheumatol 2012;8:501.
[18] Li G, Yin J, Gao J, Cheng TS, Pavlos NJ, Zhang C, et al. Subchondral bone in osteoarthritis: insight into risk factors and microstructural changes. Arthritis Res Ther 2013;15:223.
[19] Sheth NP, Lonner JH. Gowned and gloved orthopaedics E-book: introduction to common procedures. Elsevier Health Sciences; 2008.
[20] Shriram D, Praveen KG, Cui F, Yhd L, Subburaj K. Evaluating the effects of material properties of artificial meniscal implant in the human knee joint using finite element analysis. Sci Rep 2017;7:6011.
[21] Li L, Yang L, Yu F, Shi J, Zhu L, Yang X, et al. 3D printing individualized heel cup for improving the self-reported pain of plantar fasciitis. J Transl Med 2018;16:167.
[22] Shepherd DE, Seedhom BB. The 'instantaneous' compressive modulus of human articular cartilage in joints of the lower limb. Rheumatology 1999;38:124–32.
[23] Haut Donahue TL, Hull ML, Rashid MM, Jacobs CR. How the stiffness of meniscal attachments and meniscal material properties affect tibio-femoral contact pressure computed using a validated finite element model of the human knee joint. J Biomech 2003;36:19–34.
[24] Dhaher YY, Kwon T-H, Barry M. The effect of connective tissue material uncertainties on knee joint mechanics under isolated loading conditions. J Biomech 2010;43:3118–25.
[25] Ahmed AM, McLean C. In vitro measurement of the restraining role of the anterior cruciate ligament during walking and stair ascent. J Biomech Eng 2002;124:768–79.
[26] Heller MO, Bergmann G, Kassi JP, Claes L, Haas NP, Duda GN. Determination of muscle loading at the hip joint for use in pre-clinical testing. J Biomech 2005;38:1155–63.
[27] Li L, Yang X, Yang L, Zhang K, Shi J, Zhu L, et al. Biomechanical analysis of the effect of medial meniscus degenerative and traumatic lesions on the knee joint. Am J Trans Res 2019;11:542–56.
[28] Mcdermott I. Meniscal tears, repairs and replacement: their relevance to osteoarthritis of the knee. Br J Sports Med 2011;45:292–7.
[29] Mp HLG, Mazzuca SJ. Radiographic-based grading methods and radiographic measurement of joint space width in osteoarthritis. Radiol Clin N Am 2009;47:567–79.
[30] Otsuki S, Nakajima M, Okamoto Y, Oda S, Hoshiyama Y, Iida G, et al. Correlation between varus knee malalignment and patellofemoral osteoarthritis. Knee Surg Sport Traumatol Arthrosc 2016;24:176–81.
[31] Yoon KH, Lee SH, Bae DK, Park SY, Oh H. Does varus alignment increase after medial meniscectomy? Knee Surg Sport Traumatol Arthrosc 2013;21:2131–6.
[32] YJ W, J W, M D, G L, L Q. Three-dimensional magnetic resonance imaging of rat knee osteoarthritis model induced using meniscal transection. J Orthop Trans 2015;3:134–41.
[33] Englund M, Guermazi A, Lohmander SL. The role of the meniscus in knee osteoarthritis: a cause or consequence? Radiol Clin N Am 2009;47:703–12.
[34] Goldring MB. Articular cartilage degradation in osteoarthritis. Hss J Musculoskel J Hosp Spec Surg 2012;8:7.
[35] Wheatley BB, Fischenich KM, Button KD, Haut RC, Haut Donahue TL. An optimized transversely isotropic, hyper-poro-viscoelastic finite element model of the meniscus to evaluate mechanical degradation following traumatic loading. J Biomech 2015;48:1454–60.
[36] Hunter DJ, Zhang YQ, Niu JB, Tu X, Amin S, Clancy M, et al. The association of meniscal pathologic changes with cartilage loss in symptomatic knee osteoarthritis. Arthritis Rheumatol 2014;54:795–801.
[37] Sanchez C, Deberg MA, Piccardi N, Msika P, Reginster JY, Henrotin YE. Subchondral bone osteoblasts induce phenotypic changes in human osteoarthritic chondrocytes. Osteoarthr Cartil 2005;13:988–97.
[38] Zuo Q, Lu S, Du Z, Thor F, Yao J, Ross C, et al. Characterization of nano-structural and nano-mechanical properties of osteoarthritic subchondral bone. BMC Muscoskelet Disord 2016;17:367.
[39] Weber J, Koch M, Angele P, Zellner J. The role of meniscal repair for prevention of early onset of osteoarthritis. J Exp Orthop 2018;5:10.
[40] Verdonk R, Madry H, Shabshin N, Dirisamer F, Peretti GM, Pujol N, et al. The role of meniscal tissue in joint protection in early osteoarthritis. Knee Surg Sport Traumatol Arthrosc 2016;24:1763–74.
[41] Englund M, Guermazi A, Roemer FW, Aliabadi P, Yang M, Lewis CE, et al. Meniscal tear in knees without surgery and the development of radiographic osteoarthritis among middle-aged and elderly persons: the multicenter osteoarthritis study. Arthritis Rheum 2014;60:831–9.
[42] Matava MJ. Meniscal allograft transplantation: a systematic review. Clin Orthop Relat Res 2007;455:142–57.